Low-Complexity Detectors for Space-Time Block Coded Differential Spatial Modulation

Yukun Yang, Han Hai, *Member, IEEE,* Xue-Qin Jiang, *Senior Member, IEEE,* Yun Wu, Shahid Mumtaz, *Senior Member, IEEE*

***Abstract*—Space-time block coded differential spatial modulation (STBC-DSM) is a recently proposed DSM-based multiple-input-multiple-output (MIMO) transmission technique with high diversity gain. The existing low-complexity detectors for STBC-DSM can be further designed to reduce complexity. In this paper, we propose an ordered antenna index vector detector (OVD) for STBC-DSM, and an OV-low repetition detector (OV-LRD) for further simplification. The OVD detects the symbols in a designed order, and the OV-LRD fully uses the STBC structure to simplify the OVD. Simulation results show that the OVD achieves near-optimal performance, and the OV-LRD significantly reduces complexity with negligible performance loss.**

***Index Terms*—Space-time block coding, differential spatial modulation, ordered block minimum mean squared error, tree search.**

I. Introduction

SPATIAL modulation (SM) [1] is a multiple-input-multiple-output (MIMO) scheme which eliminates the inter channel interference (ICI) and inter antenna synchronization (IAS) by activating one transmit antenna at any time slot, and increases the throughput by mapping additional information bits into the indices of transmit antennas [2]. Generalized spatial modulation (GSM) [3], [4] technique is an extension of SM, which allows multiple transmit antennas to be activated at a time slot and improves the spectral efficiency. Differential spatial modulation (DSM) [5]–[7] extends SM in time domain, which transmits the information bits with the activated antenna matrix (AM) indices and equal energy constellation symbols. Each AM denotes the activation order of N_T transmit antennas in N_T consecutive time slots, which can also be represented by an antenna index (AI) vector of length N_T. DSM avoids utilizing the channel state information (CSI) by performing differential modulation and demodulation on the transmit and receive sides, which has attracted extensive research. In recent years, amplitude phase shift keying DSM (APSK-DSM) [8], reorder APSK-DSM (RPASK-DSM) [9], and absolute amplitude differential phase SM (AADP-SM) [10] have been proposed for higher transmission rates and reliability.

However, the aforementioned DSM schemes only activate one antenna per time slot. Although each AM is limited to a permutation matrix, it is possible to activate multiple antennas simultaneously. Therefore, diversity gain can be improved through careful design. To achieve the diversity gain improvement, a space-time block coded DSM (STBC-DSM) scheme is proposed in [11]. By altering the structures of AMs and symbols in conventional DSM into Alamouti's STBC, the STBC-DSM attains diversity gain with sparse radio-frequency chains at the transmitter [12]. For STBC-DSM detection, the optimal maximum likelihood detector (MLD) has the highest complexity. To reduce the complexity of STBC-DSM systems, several low-complexity detectors have been proposed. In quasi-static channels, a low-complexity noncoherent ML detector (LC-MLD) is proposed in [14], which exhaustively searches the set of Alamouti's STBC matrices. A symbol-by-symbol low-complexity detector (LCD) is proposed in [11], which has only an insignificant bit error ratio (BER) performance loss compared with the MLD. However, the part of AM detection in LCD requires amending the illegitimate initial estimated result and causes the majority of the complexity, which attracts us to further design. In time-selective channels, a decision-feedback differential detection (DFDD) based detector is proposed [13]. The DFDD is a multi-block detection, and its metric is related to a few previous detection results, mitigating the drawbacks of fast fading. Nevertheless, the complexity of DFDD is higher than that of LCD.

In [15] and [16], an ordered-block minimum mean squared error (OB-MMSE) detector for GSM systems is proposed, which firstly detects the transmit antenna combinations (TAC) by well-designed weight factors, then the possible corresponding symbol vectors are detected in sequence by the MMSE detector. The OB-MMSE detector can achieve the similar BER performance to the MLD in GSM systems. However, the accurate CSI is required for detection, which is considerably difficult and costly to obtain, resulting in an inevitable performance penalty.

Considering the above background, the major contributions of this paper can be summarized as follows:

1) We propose a two-block detector in quasi-static channels, named the ordered AI vector detector (OVD). The OVD modifies the ordering algorithm of the original OB-MMSE detector to fit the antenna detection of the STBC-DSM systems, and jointly detects the symbols of two

This work was supported by the National Natural Science Foundation of China (No. 61801106), in part by the 6G-SENSES project from the Smart Networks and Services Joint Undertaking (SNS JU) under the European Union's Horizon Europe research and innovation programme under Grant Agreement No 101139282. (Corresponding author: Han Hai.)

Y. Yang, H. Hai, X.-Q. Jiang and Yun Wu are with the College of Information Science and Technology, Donghua University, Shanghai, 201620, China (e-mail:hhai@dhu.edu.cn). Shahid Mumtaz is with the Department of Applied Informatics, Silesian University of Technology Akademicka 16 44-100 Gliwice, Poland and Nottingham Trent University, Department of Computer Sciences.

adjacent time slots. By detecting all AI vector candidates, the OVD can achieve near-optimal performance.

2) Moreover, to further reduce the complexity of the OVD, we propose an OV-low repetition detector (OV-LRD). The OV-LRD reduces the number of detected AI vector candidates, and fully utilizes the orthogonality of the STBC scheme to simplify the calculations. Simulation results show that the OV-LRD significantly reduces complexity with negligible performance loss.

The remainder of this paper is organized as follows. In Section II, a brief review of STBC-DSM is given. In Section III, the OVD and the OV-LRD are described in detail. Simulation results are given in Section IV, followed by a conclusion in Section V.

$Notations$: Upper case boldface letter $\boldsymbol{A}$ is a matrix, $\boldsymbol{A}^i$ is the i-th column of matrix $\boldsymbol{A}$, and $[\boldsymbol{A}]_{m,n}$ is the element in row m and column n of $\boldsymbol{A}$. Lower case boldface letter $\boldsymbol{a}$ is a vector, and $[\boldsymbol{a}]_m$ is the m-th element of $\boldsymbol{a}$. $\|\cdot\|$ represents the Euclidean norm of a vector. $(\cdot)^T$, $(\cdot)^*$ and $(\cdot)^H$ are used to denote the transpose, conjugate and Hermitian transpose of a vector or a matrix, respectively. $|\cdot|$ represents the magnitude of a complex quantity, $diag[\cdot]$ represents the creation of a diagonal matrix, $\lfloor\cdot\rfloor$ denotes the floor function, and $\mathbb{Q}(\cdot)$ represents the function that demodulates the input vector into constellation symbols.

II. System Model

Consider a conventional DSM system [7] with $N_T^{'}$ transmit antennas and $N_R^{'}$ receive antennas. For the conventional DSM scheme, one out of Q AMs is chosen to convey $\lfloor \log_2(N_T^{'}!) \rfloor$ bits during $N_T^{'}$ time slots, where $Q = 2^{\lfloor \log_2(N_T^{'}!) \rfloor}$. For each conventional AM $\boldsymbol{A}_q$ of size $N_T^{'} \times N_T^{'}$, $q \in (1, \ldots, Q)$, there is only one non-zero element on each row and column, such that each $\boldsymbol{A}_q$ corresponds to a certain AI vector $\boldsymbol{l}_q = (l_q^1, l_q^2, \ldots, l_q^t, \ldots, l_q^{N_T^{'}})$, where l_q^t represents the activated AI at t-th column of $\boldsymbol{A}_q$, and $t \in (1, \ldots, N_T^{'})$.

The STBC-DSM system [11] can be extended from the conventional DSM system. In an STBC-DSM system with N_T transmit antennas and N_R receive antennas, where $N_T = 2N_T^{'}$, an extended AM $\boldsymbol{G}_q$ of size $N_T \times N_T$ can be obtained by replacing each non-zero element in $\boldsymbol{A}_q$ with a 2×2 identity matrix, and each zero element with a 2×2 zero matrix. Each transmission of STBC-DSM lasts for N_T time slots. At the k-th transmission, $B_k = \lfloor \log_2[(N_T/2)!] \rfloor + N_T b$ bits are utilized to generate an STBC-DSM transmitted space-time block. The first $\lfloor \log_2[(N_T/2)!] \rfloor$ bits are mapped to one of the extended AMs $\boldsymbol{G}_q$. The rest $N_T b$ bits are utilized to modulate N_T M-PSK symbols $\boldsymbol{s} = [s_1, s_2, \ldots, s_{N_T}]$, where $M = 2^b$ is the modulation order of constellation set. Then, $N_T/2$ Alamouti's STBC matrices are generated with N_T symbols as follows

$$\boldsymbol{\mathcal{I}}_t = \frac{1}{\sqrt{2}} \begin{bmatrix} s^{2t-1} & -\left(s^{2t}\right)^* \\ s^{2t} & \left(s^{2t-1}\right)^* \end{bmatrix}, (t = 1, 2, \ldots, N_T/2). \quad (1)$$

According to the STBC-DSM scheme in [11], the k-th transmitted space-time block can be expressed as

$$\boldsymbol{S}_k = \boldsymbol{S}_{k-1} \boldsymbol{X}_k, \quad (2)$$

where $\boldsymbol{S}_0 = \boldsymbol{I}_{N_T}$, $\boldsymbol{I}_{N_T}$ is an identity matrix of size $N_T \times N_T$, and k-th information space-time block $\boldsymbol{X}_k$ can be obtained as

$$\boldsymbol{X}_k = \boldsymbol{G}_q diag\left[\boldsymbol{\mathcal{I}}_1, \boldsymbol{\mathcal{I}}_2, \ldots, \boldsymbol{\mathcal{I}}_{\frac{N_T}{2}}\right]. \quad (3)$$

The k-th received space-time block of the STBC-DSM system $\boldsymbol{Y}_k$ can be expressed as

$$\boldsymbol{Y}_k = \boldsymbol{H}_k \boldsymbol{S}_k + \boldsymbol{N}_k, \quad (4)$$

where $\boldsymbol{H}_k \in \mathbb{C}^{N_R \times N_T}$ is the channel matrix obeying the complex Gaussian distribution $\mathcal{CN}(0, 1)$, and $\boldsymbol{N}_k \in \mathbb{C}^{N_R \times N_T}$ is the noise matrix obeying $\mathcal{CN}(0, \sigma^2)$.

Assuming $\boldsymbol{H}_{k-1} \approx \boldsymbol{H}_k$ in quasi-static channels, the MLD can be expressed as

$$\hat{\boldsymbol{X}}_k = \underset{\boldsymbol{X}_k \in \mathbb{X}}{\arg\min} \left\| \boldsymbol{Y}_k - \boldsymbol{Y}_{k-1} \boldsymbol{X}_k \right\|^2, \quad (5)$$

where $\mathbb{X}$ represents the set of all possible information space-time blocks.

III. Proposed Low-complexity Detectors

In this section, the OVD and the OV-LRD for STBC-DSM are proposed, respectively. First, for the OVD, a sorting algorithm for all candidate AI vectors is designed, and a block MMSE detector is used for symbol detection. Then, based on the OVD, we proposed a complexity reduction algorithm for the OV-LRD by fully utilizing the orthogonality of the STBC structure. Finally, we analyze the complexity for both proposed detectors and other existing detectors.

A. Proposed Ordered AI Vector Detector

In the proposed OVD, the activated AI vector $\boldsymbol{l}_q$ and the transmitted symbols are detected separately for complexity reduction. Different from OB-MMSE, which detects transmit antenna combinations within a single time slot, the proposed OVD employs a weight factor to represent the probability of antenna activation during two adjacent time slots for the activated AI vector detection. Additionally, sort factors are utilized to arrange all candidate AI vectors over N_T time slots. Considering the transmitted symbols and received signal between ($2t$-1)-th and ($2t$)-th time slots, we have

$$\boldsymbol{y}_t = \frac{1}{\sqrt{2}} \boldsymbol{W}_{q,t} \begin{bmatrix} s^{2t-1} \\ s^{2t} \end{bmatrix} + \begin{bmatrix} \boldsymbol{N}_k^{2t-1} \\ (\boldsymbol{N}_k^{2t})^* \end{bmatrix}, \quad (6)$$

where $\boldsymbol{y}_t = \begin{bmatrix} \boldsymbol{Y}_k^{2t-1} \\ (\boldsymbol{Y}_k^{2t})^* \end{bmatrix}$, and

$$\boldsymbol{W}_{q,t} = \begin{bmatrix} \boldsymbol{Y}_{k-1}^{2l_q^t - 1} & \boldsymbol{Y}_{k-1}^{2l_q^t} \\ \left(\boldsymbol{Y}_{k-1}^{2l_q^t}\right)^* & -\left(\boldsymbol{Y}_{k-1}^{2l_q^t - 1}\right)^* \end{bmatrix}. \quad (7)$$

For the t-th index $\hat{l}_i^t$ of the i-th candidate AI vector $\hat{\boldsymbol{l}}_i$, the weight factor [16] can be obtained as

$$u_{i,t} = \|\boldsymbol{y}_t\|^2 - \|\boldsymbol{y}_t - \boldsymbol{W}_{i,t} \boldsymbol{s}_{est}\|^2 \quad (8)$$

where $i \in \{1, 2, \ldots, Q\}$, $\hat{\boldsymbol{l}}_i = (\hat{l}_i^1, \hat{l}_i^2, \ldots, \hat{l}_i^t, \ldots, \hat{l}_i^{N_T/2})$, and $\boldsymbol{s}_{est} = \mathbb{Q}\left[\left(\boldsymbol{W}_{i,t}^H \boldsymbol{W}_{i,t}\right)^{-1} \boldsymbol{W}_{i,t}^H \boldsymbol{y}_t\right]$. Instead of the symbol

detection result, $\boldsymbol{s}_{est}$ is introduced as a nonlinear operation to mitigate the impact of channel effects in small-scale antenna scenarios, especially when $N_R < 4$. $u_{i,t}$ represents how likely the t-th element of $\boldsymbol{l}_q$ is $\hat{l}_i^t$, where $\boldsymbol{l}_q$ represents the AI vector that is differential encoded at the transmitter. Then, a sort factor U_i of $\hat{\boldsymbol{l}}_i$ can be obtained as

$$U_i = \sum_{t=1}^{N_T/2} u_{i,t}. \tag{9}$$

After obtaining all sort factors $\boldsymbol{u} = [U_1, U_2, \ldots, U_Q]$, the sorted sequence of AI vectors can be obtained as

$$[z_1, z_2, \ldots, z_Q] = sort(\boldsymbol{u}), \tag{10}$$

where $sort(\cdot)$ represents the sorting operations on input elements in descending order, z_1 and z_Q are the indices of the maximum and minimum values in $\boldsymbol{u}$, respectively, i.e., $\hat{\boldsymbol{l}}_{z_1}$ and $\hat{\boldsymbol{l}}_{z_Q}$ have the highest and lowest possibility of being activated at the transmitter, respectively. Then, the sorted sequence of $\hat{\boldsymbol{l}}$ will be utilized in order by a block MMSE equalization processing method [15]. For the n-th sorted candidate $\hat{\boldsymbol{l}}_{z_n}$, $n \in \{1, 2, \ldots, Q\}$, the corresponding detected symbols in the ($2t$-1)-th and ($2t$)-th time slots can be obtained as

$$\left[\hat{s}_{z_n}^{2t-1}, \hat{s}_{z_n}^{2t}\right]^T = \mathbb{Q}\left[\left(\boldsymbol{W}_{z_n,t}^H \boldsymbol{W}_{z_n,t} + \sigma^2 \boldsymbol{I}_2\right)^{-1} \boldsymbol{W}_{z_n,t}^H \boldsymbol{y}_t\right], \tag{11}$$

where $\boldsymbol{I}_2$ represents an identity matrix of size 2×2. $\left[\hat{s}_{z_n}^{2t-1}, \hat{s}_{z_n}^{2t}\right]^T$ are considered as the MMSE detected symbols derived from (6). The detection for the n-th sorted candidate $\hat{\boldsymbol{l}}_{z_n}$ will be omitted when $\hat{l}_{z_n}^t$ and $\left[\tilde{s}_{z_n}^{2t-1}, \tilde{s}_{z_n}^{2t}\right]^T$ do not satisfy

$$\frac{1}{\sigma^2}\left\|\boldsymbol{y}_t - \frac{1}{\sqrt{2}}\boldsymbol{W}_{z_n,t}\left[\hat{s}_{z_n}^{2t-1}, \hat{s}_{z_n}^{2t}\right]^T\right\|^2 \leq V^{'}, \tag{12}$$

where $V^{'}$ represents a termination threshold [17]. $V^{'}$ can be obtained as

$$V^{'} = \alpha \frac{\lambda_{t,min}^2 d_{min}^2}{2\sigma^2} + 2N_R, \tag{13}$$

where α is the coefficient depending on N_T, $\lambda_{t,min}$ represents the minimum singular value of $\boldsymbol{W}_{z_n,t}$, and d_{min} represents the minimum distance between two constellation points. If all $N_T/2$ outputs of block MMSE detector satisfy (12), the N_T detected symbols can be expressed as

$$\hat{\boldsymbol{s}}_{z_n} = \left[\hat{s}_{z_n}^1, \hat{s}_{z_n}^2, \ldots, \hat{s}_{z_n}^{N_T-1}, \hat{s}_{z_n}^{N_T}\right]^T, \tag{14}$$

and the OVD will take the n-th output $\left(\hat{\boldsymbol{l}}_{z_n}, \hat{\boldsymbol{s}}_{z_n}\right)$ as the final detection output, i.e., $\hat{\boldsymbol{l}}_q = \hat{\boldsymbol{l}}_{z_n}$, $\hat{\boldsymbol{s}} = \hat{\boldsymbol{s}}_{z_n}$. Otherwise, n will be updated to $n+1$, and detection will continue with the next candidate when $n \leq Q$. If $n > Q$, the final detection output is obtained as

$$\begin{cases} \mathbb{W}_{j,t}^{'} = \left\|\boldsymbol{y}_t - \frac{1}{\sqrt{2}}\boldsymbol{W}_{z_j,t}\left[\hat{s}_{z_j}^{2t-1}, \hat{s}_{z_j}^{2t}\right]^T\right\|^2, \\ v = \arg\min\limits_{j} \sum\limits_{t=1}^{N_T/2} \mathbb{W}_{j,t}^{'},\ \hat{\boldsymbol{l}}_q = \hat{\boldsymbol{l}}_{z_v},\ \hat{\boldsymbol{s}} = \hat{\boldsymbol{s}}_{z_v}. \end{cases} \tag{15}$$

Finally, the output $\left(\hat{\boldsymbol{l}}_q, \hat{\boldsymbol{s}}\right)$ is decoded into bits.

B. Proposed Ordered AI Vector Low Repetition Detector

OVD can obtain the optimal accuracy of antenna detection by exhaustive search. However, there are plenty of multiplications of matrices and repeated calculations in the OVD, and the complexity of exhaustively searching all AI vectors is unacceptable when N_T increases. These issues attract us to propose the OV-LRD to simplify the OVD. By using the orthogonality of the STBC structure, the simplifications of each step of the OVD are formed and presented as follows. First, note that in ($2t$-1)-th and ($2t$)-th time slots, we have

$$\begin{cases} \left(\boldsymbol{W}_{i,t}^n\right)^H \boldsymbol{W}_{i,t}^m = A_{i,t}, & n = m, \\ \left(\boldsymbol{W}_{i,t}^n\right)^H \boldsymbol{W}_{i,t}^m = 0, & n \neq m, \end{cases} \tag{16}$$

where $A_{i,t} = \left\|\boldsymbol{Y}_{k-1}^{2l_i^t-1}\right\|^2 + \left\|\boldsymbol{Y}_{k-1}^{2l_i^t}\right\|^2$. Then, a large amount of computation caused during the detection process of the OVD can be simplified according to (16). For the activated AI vector detection, (6) can be considered as a GSM that activates two transmit antennas. Then, the iterative simplification technique in [16] can be employed. By replacing $\boldsymbol{s}_{est}$ with its original linear form, the process of obtaining a weight factor in (8) can be simplified as

$$\begin{aligned} u_{i,t} &\approx \|\boldsymbol{y}_t\|^2 - \|\boldsymbol{y}_t - \boldsymbol{P}_{i,t}\boldsymbol{y}_t\|^2 = \boldsymbol{y}_t^H \boldsymbol{P}_{i,t}\boldsymbol{y}_t \\ &= \frac{1}{A_{i,t}}\left[\left|\left(\boldsymbol{W}_{i,t}^1\right)^H \boldsymbol{y}_t\right|^2 + \left|\left(\boldsymbol{W}_{i,t}^2\right)^H \boldsymbol{y}_t\right|^2\right] \end{aligned} \tag{17}$$

where $\boldsymbol{P}_{i,t} = \boldsymbol{W}_{i,t}(\boldsymbol{W}_{i,t}^H \boldsymbol{W}_{i,t})^{-1}\boldsymbol{W}_{i,t}^H$. It is noted that $u_{i,t}$ is related to the AI $\hat{l}_i^t$ and time slot t, which means the maximum number of different values for $u_{i,t}$ is $N_T/2 \times N_T/2$. Set matrix $\boldsymbol{U}$ of size $N_T/2 \times N_T/2$ to store all possible values of weight factors, where $[\boldsymbol{U}]_{l,t}$ represents the weight factor of AI l in $(2t-1)$-th and $(2t)$-th time slots, and $l \in \{1, \ldots, N_T/2\}$. Then, the sort factor of $\hat{\boldsymbol{l}}_i$ can be obtained by accumulating $[\boldsymbol{U}]_{\hat{l}_i^t,t}$ for $t = 1, \ldots, N_T/2$.

However, the accumulation executes for all Q AI vectors in the OVD, while the final detection output is obtained after a few candidates are detected. Therefore, in the proposed OV-LRD, the number of candidates for detection is reduced. First, we use the well-known Kuhn-Munkres algorithm [18] to directly choose the first AI vector candidate. In order to utilize the Kuhn-Munkres algorithm, $\boldsymbol{U}$ is transformed into a bipartite graph, where one set of vertices represents the time slots, the other set represents the antennas, and the cost of each edge is the element of $\boldsymbol{U}$. Then, the Kuhn-Munkres algorithm can efficiently find the optimal matching $\hat{\boldsymbol{l}}_{KM}$ with a complexity of $\mathcal{O}(N_T^3)$. The $\hat{\boldsymbol{l}}_{KM}$ can be regarded as the AI vector that maximizes the sorted factor in (9), i.e., $\hat{\boldsymbol{l}}_{KM}$ is the first candidate to detect symbols in the OV-LRD. $\hat{\boldsymbol{l}}_{KM}$ is most likely to be activated at the transmitter, especially at high signal-to-noise ratio (SNR). However, due to the possible situations where the $\hat{\boldsymbol{l}}_{KM}$ does not satisfy the termination condition or is not one of the Q AI vectors, it is necessary to consider additional candidates. A sphere-based tree search algorithm (TS_ρ) proposed in [19] is modified in this paper and utilized to choose additional candidates when the $\hat{\boldsymbol{l}}_{KM}$ can not terminate the OV-LRD. TS_ρ turns the calculation of sort factors into a breadth-first tree search with N_T layers. A

Algorithm 1 The KM aided TSρ

Input: $N_T, \hat{\boldsymbol{l}}_{KM}$, $\boldsymbol{U}$ and radius ρ.
Output: All chosen AI vector candidates $\hat{\boldsymbol{L}}_c$ and candidate number N_L.

set $\boldsymbol{d} = \left[d_1, d_2, \ldots, d_{N_T/2}\right]$, $d_i = [\boldsymbol{U}]_{1,i}$;
set $\boldsymbol{L} = [1, 2, \ldots, N_T/2]$;
for $t = 2$ to $N_T/2$ **do**
  set $\boldsymbol{d}_c = \emptyset, \boldsymbol{L}_c = \emptyset, N = length(\boldsymbol{d})$;
  set $\boldsymbol{p} = \left\{ i \mid i \in \{1, \ldots, N\}, d_i - d_{[\boldsymbol{l}_{\boldsymbol{KM}}]_{t-1}} \leq \rho \right\}$;
  for $i = 1$ to $length(\boldsymbol{p})$ **do**
    set $\boldsymbol{c} = \left\{ j \mid j \in \{1, \ldots, N_T/2\}, j \notin \boldsymbol{L}^{[\boldsymbol{p}]_i} \right\}$;
    for $j = 1$ to $length(\boldsymbol{c})$ **do**
      $\boldsymbol{d}_c = \left[\boldsymbol{d}_c, d_i + [\boldsymbol{U}]_{[\boldsymbol{c}]_j, t}\right]$;
      $\boldsymbol{L}_c = \left[\boldsymbol{L}_c, \left[\left(\boldsymbol{L}^{[\boldsymbol{p}]_i}\right)^T, [\boldsymbol{c}]_j\right]^T\right]$;
    end for
  end for
  update $\boldsymbol{d} = \boldsymbol{d}_c, \boldsymbol{L} = \boldsymbol{L}_c$;
end for
set $N_L = length(\boldsymbol{d}_c)$;
ordering the rows of $\boldsymbol{L}_c^T$ in descending order based on the elements of $\boldsymbol{d}_c$ to obtain $\hat{\boldsymbol{L}}_c$.

node with a number l at the t-th layer represents the AI l at the t-th time slot, and the current metric corresponding to this node d_c is obtained as $d_c = d + [\boldsymbol{U}]_{l,t}$, where d represents the metric of the parent node. The nodes at the t-th layer that satisfy $d_c - d_{KM,t} \leq \rho$ will be expanded, where $d_{KM,t}$ is the metric of the node that represents the t-th AI of $\hat{\boldsymbol{l}}_{KM}$, and ρ is a predefined radius. The child nodes of an expanded node consist of antenna indices that have not been accessed on the path from the root node to the current node. Specifically, the modified TS_ρ is summarized in **Algorithm 1**, where $length(\cdot)$ outputs the length of the input vector. At the end of the modified TS_ρ, the paths from the root node to all leaf nodes at the N_T layer are considered as additional candidates, and the rows of matrix $\hat{\boldsymbol{L}}_c$ represent these additional candidates. N_L represents the number of additional candidates, which is adjusted by the radius ρ.

For the transmitted symbol detection, according to (16), $\boldsymbol{W}_{z_n,t}^H \boldsymbol{W}_{z_n,t} = A_{z_n,t} \boldsymbol{I}_2$. Then, the block MMSE detector in (11) can be simplified as

$$\begin{aligned}[\hat{s}_{z_n}^{2t-1}, \hat{s}_{z_n}^{2t}]^T &= \mathbb{Q}\left\{ \frac{1}{A_{z_n,t} + \sigma^2} \left[\left(\boldsymbol{W}_{z_n,t}\right)^H \boldsymbol{y}_t \right]^T \right\} \\ &= \mathbb{Q}\left\{ \frac{1}{A_{z_n,t} + \sigma^2} \left[\left(\boldsymbol{W}_{z_n,t}^1\right)^H \boldsymbol{y}_t, \left(\boldsymbol{W}_{z_n,t}^2\right)^H \boldsymbol{y}_t \right]^T \right\}. \end{aligned} \tag{18}$$

And for the termination threshold comparison, by left multiplying $\left(\boldsymbol{W}_{z_n,t}\right)^H$, (12) can be simplified as

$$\frac{1}{\sigma^2} \left\| \left(\boldsymbol{W}_{z_n,t}\right)^H \boldsymbol{y}_t - \frac{A_{z_n,t}}{\sqrt{2}} \begin{bmatrix} \hat{s}_{z_n}^{2t-1} \\ \hat{s}_{z_n}^{2t} \end{bmatrix} \right\|^2 \leq V_{z_n,t} \tag{19}$$

where $V_{z_n,t}$ is the threshold of the t-th symbol detection of the candidate $\hat{\boldsymbol{l}}_{z_n}$. According to the compatibility of norms,

TABLE I
THE COMPLEXITY OF DIFFERENT DETECTORS

Detector	Complexity
MLD	$C_{MLD} = 8N_T^2 N_R \times Q \times 2^{N_T b}$
LC-MLD	$C_{LC-MLD} = (16N_T N_R \times 2^{2b} + N_T/2 - 1) \times Q$
LCD	$C_{LCD} = (112N_R - 8) \times (N_T/2)^2 + p_{il}(8N_T^2 N_R + 32N_T N_R - 3N_T)\hat{Q}_M$
proposed OVD	$C_{OVD} = (20N_R - 2) \times \frac{N_T}{2} + (144N_R - 3) \times \frac{N_T}{2} Q + (232N_R + 3) \times P_{avg}$
proposed OV-LRD	$C_{OV-LRD} = 8N_T^2 N_R - + N_T(8N_R - 2) + \mathcal{O}(N_T^3) + 2p_{il} P_{node} + 28P_{avg}$

$V_{z_n,t}$ can be obtained as

$$\begin{aligned} &\frac{1}{\sigma^2} \left\| \left(\boldsymbol{W}_{z_n,t}\right)^H \boldsymbol{y}_t - \frac{A_{z_n,t}}{\sqrt{2}} \left[\hat{s}_{z_n}^{2t-1} \hat{s}_{z_n}^{2t}\right]^T \right\|^2 \\ &\leq \frac{1}{\sigma^2} \left\|\boldsymbol{W}_{z_n,t}\right\|^2 \left\| \boldsymbol{y}_t - \frac{1}{\sqrt{2}} \boldsymbol{W}_{z_n,t} \left[\hat{s}_{z_n}^{2t-1} \hat{s}_{z_n}^{2t}\right]^T \right\|^2 \\ &\leq A_{z_n,t} \left(\alpha \frac{A_{z_n,t} d_{min}^2}{2\sigma^2} + 2N_R \right) = V_{z_n,t}. \end{aligned} \tag{20}$$

Note that $A_{z_n,t}$ and the inner products of $\left(\boldsymbol{W}_{z_n,t}\right)^H \boldsymbol{y}_t$ appear several times in the detection process of the OV-LRD. Therefore, the complexity can be further reduced by storing these repeated computations. At the beginning of OV-LRD, $\boldsymbol{\Upsilon}$ and $\boldsymbol{\gamma}$ are set as the storage. The reduction algorithm saves the values of $\left(\boldsymbol{W}_r^1\right)^H \boldsymbol{y}_m$ as $[\boldsymbol{\Upsilon}]_{2r-1,m}$, $\left(\boldsymbol{W}_r^2\right)^H \boldsymbol{y}_m$ as $[\boldsymbol{\Upsilon}]_{2r,m}$, and $\left\|\boldsymbol{Y}_{k-1}^{2r-1}\right\|^2 + \left\|\boldsymbol{Y}_{k-1}^{2r}\right\|^2$ as $[\boldsymbol{\gamma}]_r$, respectively, where $\boldsymbol{W}_r$ is the simplified representation of $\boldsymbol{W}_{q,t}$, consisting of $\boldsymbol{Y}_{k-1}^{2r-1}$ and $\boldsymbol{Y}_{k-1}^{2r}$. Then, for weight factor calculation in (17), $A_{i,t}$ can be replaced by $[\boldsymbol{\gamma}]_{\hat{l}_i^t}$, $\left(\boldsymbol{W}_{i,t}^1\right)^H \boldsymbol{y}_t$ can be replaced by $[\boldsymbol{\Upsilon}]_{2\hat{l}_i^t - 1, t}$, and $\left(\boldsymbol{W}_{i,t}^2\right)^H \boldsymbol{y}_t$ can be replaced by $[\boldsymbol{\Upsilon}]_{2\hat{l}_i^t, t}$. Similar replacements can be applied in (18), (19) and (20). It is worth highlighting that $\hat{l}_i^t$ is essentially a number determined by the i-th AI vector candidate and the t-th time slot, representing a specific AI. After substituting with the stored values into the OV-LRD detection process, a large number of complex multiplications are omitted, the computations of computing weight factors and detecting symbols only consist of additions and multiplications among real numbers, and are independent of system parameters.

C. Complexity Analysis

In this letter, the complexity of a detector is evaluated in terms of the number of real floating point operations (flops) needed by demodulating one space-time block, where flops consist of real-valued additions and real-valued multiplications. Flops can analyze the complexity more comprehensively than using real-valued multiplications alone. **TABLE I** summaries the complexity of both proposed detectors and other existing detectors for STBC-DSM, where P_{avg} represents the average implementation times of the symbol detection described in (11) and (12) for the OVD, and the simplified symbol detection described in (18) and (19) for the OV-LRD, respectively. P_{node} represents the average number of nodes accessed for the modified TS_ρ. p_{il} represents the average probability of the illegitimate initial estimated AI vector for LCD and proposed detectors, and $\hat{Q}_M$ represents the number of AI vectors converted from the illegitimate initial estimated AI vector in the LCD.

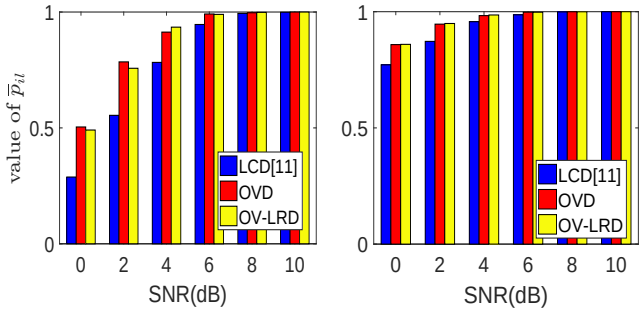

Fig. 1. The accuracy of initially detecting the activated AI vector for the proposed detectors and the LCD. (a) $N_T = 4$, $N_R = 4$, QPSK, (b) $N_T = 8$, $N_R = 4$, QPSK.

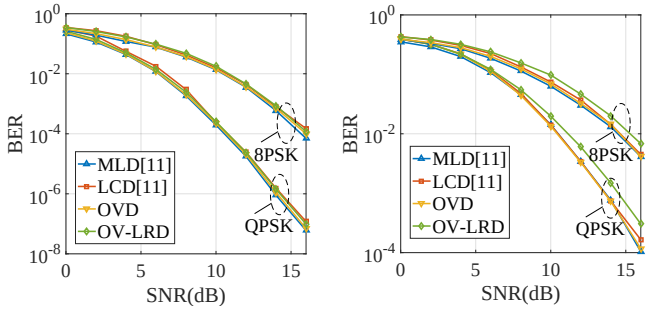

Fig. 2. BER performance comparison among various detectors for the STBC-DSM systems. (a) $N_T = 8, N_R = 4$, (b) $N_T = 8, N_R = 2$.

Specifically, in the proposed OVD, obtaining $\|\boldsymbol{y}_t\|^2$ involves $2N_R$ complex multiplications (CM) and $2N_R - 1$ complex additions (CA), and there are $N_T/2$ different $\|\boldsymbol{y}_t\|^2$. Then, obtaining $\boldsymbol{s}_{est}$ in (8) involves $12N_R$ CM and $12N_R - 6$ CA, and the inverse of the 2x2 matrix $\boldsymbol{W}_{i,t}^H \boldsymbol{W}_{i,t}$ requires 9 flops. Further, obtaining $\|\boldsymbol{y}_t\|^2 - \|\boldsymbol{y}_t - \boldsymbol{W}_{i,t}\boldsymbol{s}_{est}\|^2$ requires $6N_R$ CM and $6N_R - 1$ CA. For the detection of all AI vectors, $(20N_R - 2) \times \frac{N_T}{2} + (144N_R - 3) \times \frac{N_T}{2}Q$ flops are needed. Implementing the block MMSE equalization in (11) requires $20N_R$ CM, $16N_R - 6$ CA, a 2×2 matrix inverse, and 4 flops for adding $\sigma^2 \boldsymbol{I}_2$. Equation (12) requires $6N_R$ CM and $6N_R - 1$ CA, and obtaining $V^{'}$ requires $4N_R$ CM and $2N_R - 1$ CA. For symbol detection, $(232N_R + 3) \times P_{avg}$ flops are needed.

In the proposed OV-LRD, obtaining storage $\boldsymbol{\Upsilon}$ requires $2N_R$ CM and $2N_R - 1$ CA for each element, $\boldsymbol{\gamma}$ requires N_R CM and $N_R - 1$ CA for each element, and weight factor storage $\boldsymbol{U}$ requires 4 flops for each element. To obtain all storage, $8N_T^2 N_R + N_T(8N_R - 2)$ flops are needed. The Kuhn-Munkres algorithm has a complexity of $\mathcal{O}(N_T^3)$, where the specific value is counted during simulation. The TS_ρ requires $2P_{node}$ flops to complete the tree search. To obtain AI vector candidates for detection, $\mathcal{O}(N_T^3) + 2p_{il}P_{node}$ flops are needed. After substituting with the stored values, implementing the simplified block MMSE equalization in (18) requires 4 flops. Equation (19) requires 19 flops, and obtaining $V_{z_n,t}$ requires 5 flops. For symbol detection, $28P_{avg}$ flops are needed.

The complexity of the proposed detectors and LCD requires statistical information obtained during simulations. Therefore, a comparison of complexity among the 5 detectors in **TABLE I** will be presented in detail in the following section.

IV. Simulation Results

In this section, we present the Monte Carlo simulation results of the proposed OVD and OV-LRD for the STBC-DSM systems. The complexity and the BER performance are taken into account when comparing the MLD, the LCD proposed in [11] and the LC-MLD proposed in [14]. All simulations run over the quasi-static Rayleigh fading channels. And the ρ of OV-LRD is set to 2.5 for all simulations.

Fig. 1 compares the accuracy of initially detecting the activated AI vector for the proposed detectors and the LCD under the configurations of $N_T = 4$, $N_R = 4$, QPSK and $N_T = 8$, $N_R = 4$, QPSK, respectively, where the accuracy $\overline{p}_{il} = 1 - p_{il}$.It can be observed that the proposed detectors show a smaller decrease in $\overline{p}_{il}$ at low SNR compared to the LCD as N_T increases. Moreover, the $\overline{p}_{il}$ of the proposed detectors increases faster with SNR than that of the LCD, leading to earlier termination of detection and reduced complexity. When comparing the two proposed detectors, since the Kuhn-Munkres algorithm possibly fails to detect one of the Q candidates as the optimal matching, OV-LRD has a slightly lower $\overline{p}_{il}$ than OVD at low SNR. At high SNR, $\overline{p}_{il}$ of both OVD and OV-LRD tends to be similar.

Fig. 2 compares the BER performance of different detectors under different modulation orders with $N_T = 8$, $N_R = 4$, and $N_T = 8$, $N_R = 2$, respectively. As shown in Fig. 2 (a), the MLD has the optimal performance. The BER performance of the proposed OVD is nearly identical to that of MLD, since the OVD detect all AI vector candidates for optimal accuracy. At low SNR, the BER performance of the proposed OV-LRD underperforms the OVD because of the reduced number of detected AI vector candidates. However, the BER performance of both proposed detectors approaches closely at high SNR, since $\overline{p}_{il}$ reaches 100%. The LCD differs from the MLD by about 0.8 dB for the QPSK, while the OV-LRD has a performance loss of only 0.4 dB when compared to the MLD. The performance loss of LCD and OV-LRD compared to MLD increases with the increase in modulation order, yet OV-LRD has less performance degradation compared to LCD in general. As shown in Fig. 2(b), since the nonlinear operation introduced in (8), OVD still has the BER performance similar to MLD when $N_R = 2$. Nevertheless, OVLRD shows a reduced ability to alleviate interference in small-scale antenna scenarios due to the approximation in (17). Therefore, when $N_R < 4$, we let OVLRD finish after obtaining two candidates $\hat{\boldsymbol{l}}_{z_a}$ and $\hat{\boldsymbol{l}}_{z_b}$ that all elements satisfy (19). Then, the OV-LRD chooses the candidate with the smaller value of $\sum_{t=1}^{N_T/2} \mathbb{W}_{j,t}$ and its corresponding detected symbols as the final output, where $\mathbb{W}_{j,t}$ is the left form of the inequality (19), and $j \in \{z_a, z_b\}$. As can be seen from Fig. 2(b), the performance of OV-LRD degrades about 1 dB compared to LCD for both QPSK and 8PSK when $N_R = 2$.

Fig. 3 confirms the performance of the OV-LRD for QPSK

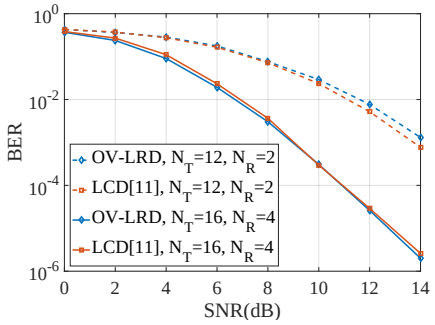

Fig. 3. BER performance comparison between LCD and OV-LRD for the STBC-DSM systems with QPSK.

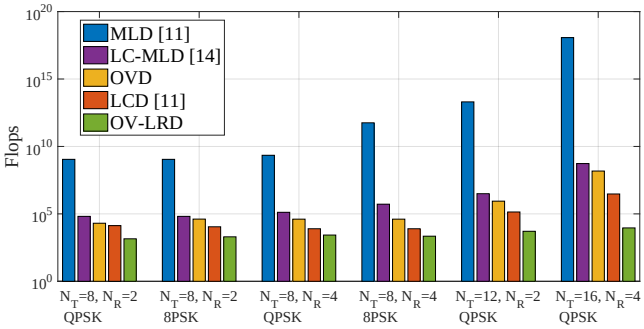

Fig. 4. Complexity comparison among various detectors for the STBC-DSM systems, SNR=0dB.

with $N_T = 12, N_R = 2$ and $N_T = 16, N_R = 4$ configurations. As expected, OV-LRD outperforms LCD at low SNR by about 0.3 dB when $N_R = 4$, and the performance of OV-LRD degrades less than 0.5dB at high SNR when $N_R = 2$.

Fig. 4 compares the complexity of various detectors with different system parameters when SNR = 0 dB. The value of ρ for OV-LRD is set to 2.5 for all configurations. For each configuration, the OVD shows almost one order of magnitude lower complexity than the LC-MLD. However, the complexity of OVD exceeds that of LCD due to the majority computation of weight factors for all candidates. At low SNR, when the first candidate fails to terminate the detection, the LCD further detects much more candidates, while the OV-LRD maintains a lower number of candidates restricted by the small radius ρ. As shown in Fig. 4, OV-LRD reduces the complexity by about one order of magnitude compared to LCD for 4 configurations on the left, and almost two orders of magnitude lower than that of LCD in large-scale transmit antenna scenarios. At high SNR, the LCD has significantly lower complexity since the detection terminates after the first candidate is detected, while OV-LRD still reduces the complexity by about 67% compared to the LCD for all configurations.

V. Conclusion

In this letter, we propose two low-complexity detectors, the OVD and the OV-LRD for the STBC-DSM systems. The detection process of the OVD is based on the modified ordering algorithm for STBC-DSM AI vector detection and the MMSE detector for symbol detection. Then, the orthogonality of the STBC structure is fully utilized in the OV-LRD to simplify all steps of the OVD. Simulation results show that the OVD can provide near-optimal BER performance, and the OV-LRD can reduce the complexity considerably with negligible performance loss compared with the other existing low-complexity detectors for the STBC-DSM systems.

References

[1] R. Y. Mesleh, H. Haas, S. Sinanovic, C. W. Ahn and S. Yun, "Spatial modulation," *IEEE Trans. Veh. Technol.*, vol. 57, no. 4, pp. 2228-2241, July 2008.

[2] M. Wen, B. Zheng, K. J. Kim, M. Renzo, T. A. Tsiftsis, K.-C. Chen, and N. Al-Dhahir, "A Survey on Spatial Modulation in Emerging Wireless Systems: Research Progresses and Applications," *IEEE J. Sel. Areas Commun.*, vol. 37, no. 9, pp. 1949-1972, Sep. 2019,

[3] A. Younis, N. Serafimovski, R. Mesleh and H. Haas, "Generalised spatial modulation," in *Proc. ASILOMAR*, Pacific Grove, CA, USA, Nov. 2010, pp. 1498-1502.

[4] J. Wang, S. Jia and J. Song, "Generalised spatial modulation system with multiple active transmit antennas and low complexity detection scheme," *IEEE Trans. Wireless Commun.*, vol. 11, no. 4, pp. 1605-1615, Apr. 2012.

[5] Y. Bian, M. Wen, X. Cheng, H. V. Poor and B. Jiao, "A differential scheme for spatial modulation," in *Proc. IEEE Global Commun. Conf.*, Atlanta, GA, USA, Dec. 2013, pp. 3925-3930.

[6] M. Wen, Z. Ding, X. Cheng, Y. Bian, H. V. Poor and B. Jiao, "Performance analysis of differential spatial modulation with two transmit antennas," *IEEE Commun. Lett.*, vol. 18, no. 3, pp. 475-478, Mar. 2014.

[7] Y. Bian, X. Cheng, M. Wen, L. Yang, H. V. Poor and B. Jiao, "Differential spatial modulation," *IEEE Trans. Veh. Technol.*, vol. 64, no. 7, pp. 3262-3268, July 2015.

[8] J. Liu, L. Dan, P. Yang, L. Xiao, F. Yu and Y. Xiao, "High-rate APSK-aided differential spatial modulation: design method and performance analysis," *IEEE Commun. Lett.*, vol. 21, no. 1, pp. 168-171, Jan. 2017.

[9] L. Yang, H. Xiu, D. Yu, P. Gao and G. Yue, "Reordered amplitude phase shift keying aided differential spatial modulation: DFDD-based low-complexity detector and performance analysis over fading channels," *IEEE Trans. Wireless Commun.*, vol. 21, no. 10, pp. 7913-7925, Oct. 2022.

[10] D. Yu, G. Yue, A. Liu and L. Yang, "Absolute amplitude differential phase spatial modulation and its non-coherent detection under fast fading channels," *IEEE Trans. Wireless Commun.*, vol. 19, no. 4, pp. 2742-2755, Apr. 2020.

[11] L. Xiao, Y. Xiao, P. Yang, J. Liu, S. Li and W. Xiang, "Space-time block coded differential spatial modulation," *IEEE Trans. Veh. Technol.*, vol. 66, no. 10, pp. 8821-8834, Oct. 2017.

[12] C. Wu, Y. Xiao, L. Xiao, P. Yang and X. Lei, "Space-time block coded rectangular differential spatial modulation," in *Proc. IEEE Int. Conf. Commun. (ICC)*, Kansas City, MO, USA, May 2018, pp. 1-6.

[13] H. Xiu, L. Yang, D. Yu, P. Gao, Z. Li, Q. Song, and G. Yue, "A DFDD based detector for space-time block coded differential spatial modulation under time-selective channels," *IEEE Commun. Lett.*, vol. 26, no. 2, pp. 359-363, Feb. 2022.

[14] R. -Y. Wei, S. -L. Chen, Y. -H. Lin and B. -C. Chen, "Bandwidth-efficient generalized differential spatial modulation," *IEEE Trans. Veh. Technol.*, vol. 72, no. 1, pp. 601-610, Jan. 2023.

[15] Y. Xiao, Z. Yang, L. Dan, P. Yang, L. Yin and W. Xiang, "Low-complexity signal detection for generalized spatial modulation," *IEEE Commun. Lett.*, vol. 18, no. 3, pp. 403-406, Mar. 2014.

[16] C. E. Chen, C. H. Li and Y. H. Huang, "An improved ordered-block MMSE detector for generalized spatial modulation," *IEEE Commun. Lett.*, vol. 19, no. 5, pp. 707-710, May 2015.

[17] X. Wu, J. S. Thompson and A. M. Wallace, "An improved sphere decoding scheme for MIMO systems using an adaptive statistical threshold," in *Proc. 17th European Signal Processing Conference (EUSIPCO)*, Glasgow, Scotland, Aug. 2009, pp. 2668-2672.

[18] W. H. Kuhn, "The hungarian method for the assignment problem," in *Naval Research Logistics Quarterly*, vol. 2. Hoboken, NJ, USA: Wiley, 1955, pp. 83–97, doi: 10.1002/nav.3800020109.

[19] M. Alshawaqfeh, A. Gharaibeh and R. Mesleh, "Tree-search-based optimal and suboptimal low complexity detectors for differential space shift keying MIMO system," *IEEE Trans. Wireless Commun.*, vol. 22, no. 3, pp. 1980-1991, Mar. 2023.